On UWB Capacity with Respect to Different Pulse Waveforms

Mohammed Abdel-Hafez, **Fatih Alagöz**[†], **Matti Hämäläinen**[††], and **Matti Latva-Aho**[††]
United Arab Emirates University, Department of Electrical Engineering, P.O.BOX 17555, Al-Ain, United Arab Emirates,
Email: mhafez@uaeu.ac.ae
[†]Department of Computer Engineering, Bogazici University, P.K. 2 TR-34342 Bebek, Istanbul, Turkey,
Email: alagoz@boun.edu.tr
[††]University of Oulu, Centre for Wireless Communications, Tutkijantie 2 E, FIN-90014, Finland,
Email: {matti.hamalainen,matla}@ee.oulu.fi

***Abstract*—This paper investigates the channel capacity with respect to pulse waveform of M-ary pulse position modulation (PPM) ultra wideband (UWB) communication systems over multiple-access and additive white Gaussian noise (AWGN) channel. Based on Gaussian approximation for the multiple access interference, an expression of the signal-to-noise ratio is derived for the UWB system using various forms of pulses. In addition to rectangular pulse, 2nd derivative Gaussian, and Rayleigh pulses are considered. The effect of pulse selection on the UWB capacity is investigated in AWGN multiuser channel. The information theoretic capacity of the UWB system is expressed as a function of system parameters. Analytical and simulation results show that the capacity of UWB system is highly influenced by the selected pulse shape.**

***Keywords*—Ultra wideband communications (UWB), M-ary-PPM, Information Capacity, Multiple-Access.**

I. INTRODUCTION

Ultra wideband (UWB) systems will soon appear in the communications marketplace. This new transmission system offers promising capabilities for short-range communications, ground and object penetrating radar, vehicular radar, security systems and other applications including D-wall and medical imaging systems, surveillance systems.etc. Moreover, this technology has the potential to deliver high data rates with very low power densities. The original UWB systems are characterized by the transmission of series of sub-nanosecond pulses (monocycles) that spread the energy of the signal from near DC to a few GHz. The current spectrum allocated by US Federal Communications Commissions (FCC) is from 3.1GHz to 10.6 GHz. The pulse train is transmitted without any modulation with sinusoidal carrier. This is one of the major advantages of UWB since it has high immunity against multipath fading effect as experienced in other wireless systems. In addition, high processing gain and very low power density ensure minimal mutual interference between the UWB and other wireless systems. Pulse position modulation (PPM) has been proposed as a modulation scheme suitable for the UWB communications [1]. With PPM, the data modulates the position of the transmitted pulse within an assigned window in time. UWB radio is the generic term describing radio systems having very large bandwidths; "bandwidths greater than 20% of the center frequency measured at the –10dB points," and "RF bandwidth greater than 500 MHz," are the two of the definitions under consideration by FCC [2].

In this paper, Time Hopping (TH) is used in the UWB system as the multiple-access method. The PPM scheme is used in TH-mode with pulse transmission instants defined by a pseudo random code. One data bit is spread over multiple pulses to achieve a processing gain due to the pulse repetition. The processing gain is increased by the low duty cycle. The multiple-access interference (MAI) may be the dominant factor on the bit error rate (BER) performance. In this paper we compute the information theoretic capacity of an UWB system with respect to different wave forms and multiuser M-ary PPM modulation. Some published works considered the information capacity for UWB system with rectangular pulse shape [5]. The correlation properties and the frequency spectra of UWB pulses are very crucial. For example, the effect of Hermite pulses on the BER performance is presented in [7]. A detailed study of PPM capacity in Gaussian and Webb channels is considered in [8]. Our paper is different from previous studies by introducing the effect of pulse shape on the information capacity of multiuser UWB system.

The remainder of this paper is organized as follows. Section 2 introduces the signal, channel, and receiver models. Section 3 carries out the system analysis for three types of waveforms; namely, Rectangular, Rayleigh and the 2nd derivative Gaussian pulses. Section 4 presents the capacity analysis of the UWB M-ary PPM in multi-user and Gaussian channel. Section 5 presents the numerical results obtained. Section 6 concludes this study.

II. UWB SYSTEM MODEL

The time-hopping M-ary PPM system model examined in this paper is shown in Fig. 1. The v-th user's transmitted signal has the form [1]:

$$S^{v}(t)=\sum_{j=-\infty}^{\infty} A^{v} P\left(t-jT_{f}-C_{j}^{v}T_{C}-d_{j}^{v}\right) \quad (1)$$

where $P(t)$ is the UWB pulse of duration T_p. The pulse repetition interval, referred to as frame, is T_f, $A^{v}=\sqrt{E_{p}^{v}}$, C_{j}^{v}, and d_{j}^{v} are respectively, the amplitude, user dependent time-hopping code and data modulation for user v, where E_p is the energy per pulse. The PPM time shift is $d_{j}^{v}\in\{\delta_{1},...,\delta_{M}\}$, Fig. 2. For a fixed T_f, the symbol rate

$R_s = 1/(N_p T_f)$ where N_p is the number of pulses that form one symbol. The symbol duration is $T_s = N_p T_f$ and, the spreading ratio is defined by $\beta = T_f / T_p$.

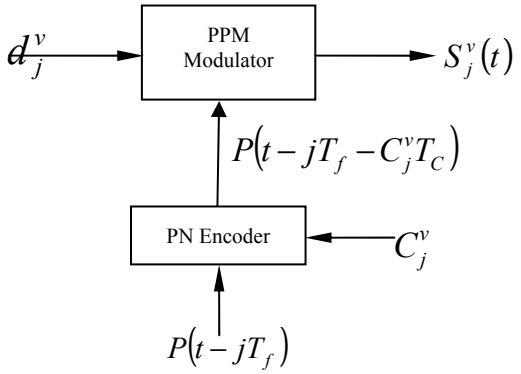

Fig. 1. TH-PPM UWB modulator.

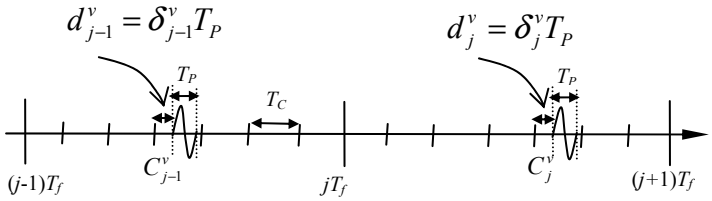

Fig. 2. Example of TH-PPM asynchronous format.

Each user's signal propagates over a single path channel with attenuation factor α and propagation delay τ. The received signal $R(t)$ from all users is given by:

$$R(t) = \sum_{v=1}^{N_u} \alpha_v S^v(t - \tau^v) + \eta(t) \qquad (2)$$

where α_v and τ^v are the channel attenuation and time delay associated with user v out of total number of N_u users, respectively, and $n(t)$ is zero-mean AWGN with power spectral density $N_0/2$.

III. UWB SYSTEM MODEL

Without loss of generality, we assume the desired user is v=1. The single-user optimal receiver is M-ary pulse correlation receiver followed by a detector. We also assume that the receiver is perfectly synchronized to user 1, i.e., τ^1 is known. Furthermore, the time hopping sequence C_j^1 is known at the receiver. The M-ary correlation receiver for user 1 consists of M filters matched to the basis function $\phi_i^1(t)$ defined as:

$$\phi_i^1(t) = P(t - d_i^1 - \tau^1) \qquad i = 1..M \quad . \qquad (3)$$

Fig. 3 depicts the detector selecting the Max i-th symbols of M possible outputs.

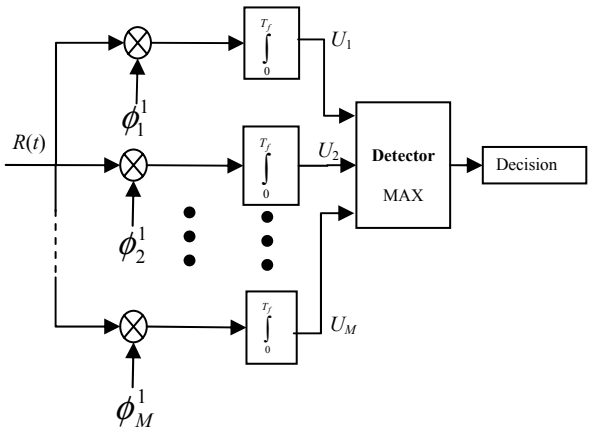

Fig. 3. M-ary PPM UWB receiver for the 1st user.

The decision variables at time sample ($t=jT_f$), are now given by:

$$U_i = \int_{(j-1)T_f}^{jT_f} R(t)\phi_j^1(t - jT_f - C_j^1 T_c)dt \qquad (4)$$

by substituting for $R(t)$ from (2), the parameter U_i can be represented as $U_i = d + MAI + N$, where d denotes the desired part of the received signal, MAI the multiple access interference from other users and is the noise component at the output of the receiver all respectively expressed by:

$$d = \int_{(j-1)T_f}^{jT_f} \alpha_1 S^1(t - \tau^1)\phi_i^1(t - jT_f - C_j^1 T_c)dt \quad , \quad (5)$$

$$MAI = \int_{(j-1)T_f}^{jT_f} \sum_{v=2}^{N_u} \alpha_v S^v(t - \tau^v)\phi_i^1(t - jT_f - C_j^1 T_c)dt \quad , \quad (6)$$

and

$$N = \int_{(j-1)T_f}^{jT_f} \eta(t)\phi_i^1(t - jT_f - C_j^1 T_c)dt \quad . \quad (7)$$

With $P(t)$ being normalized and orthogonal pulses, the desired part of the signal is $d = \alpha_1 A^1 \delta(i - j)$. The MAI part can be written as $MAI = \sum_{v=2}^{N_u} \alpha_v A^v \int_0^{T_f} P(t)P(t - \Delta)dt$, where Δ is the time difference between the different users expressed as $\Delta = (C_j^1 - C_j^v) - (d_i^1 - d_j^v) - (\tau^1 - \tau^v)$.

If the correlation function of the pulse $P(t)$ is defined by:

$$h(\Delta) = \int_0^{T_f} P(t)P(t - \Delta)dt \qquad (8)$$

then the expression for MAI in can be written as:

$$MAI = \sum_{v=2}^{N_u} \alpha_v A^v h(\Delta) \quad . \qquad (9)$$

It is assumed that all the time-hopping code elements j are random and independent, uniformly distributed over a frame interval T_f for all users and frames. Each user has a uniformly distributed data source. The time delays are also assumed

random, i.i.d. uniformly distributed over the frame interval. Under the assumptions listed above, and noting that MAI pulses of interest fall within the same UWB frame, the time difference Δ is a uniformly distributed random variable over the interval $[-T_f, T_f]$.

Various waveforms with complex mathematical formats have been proposed for impulse radio including Gaussian pulse, Gaussian monocycle [1], and Rayleigh monocycle [7]. All of these waveforms reflect the high-pass-filtering impact of the transmitter and receiver antennas. To simplify our analysis, we consider three types of waveforms; namely, Rectangular, Rayleigh and the 2nd derivative Gaussian pulses. These waveforms are presented in Fig. 4. This analysis can be extended to other waveforms that satisfy the FCC mask.

We assume the following *rectangular waveform*:

$$P_{rect}(t)=\begin{cases}\sqrt{\dfrac{1}{T_P}} & 0\le t\le T_P\\ 0 & \text{Otherwise}\end{cases}. \qquad (10)$$

The correlation function $h(\Delta)$ for $P_{rect}(t)$ in (15) is:

$$h_{rect}(\Delta)=\begin{cases}1-\dfrac{|\Delta|}{T_P} & 0\le|\Delta|\le T_b\\ 0 & \text{Otherwise}\end{cases}. \qquad (11)$$

Comparing with a rectangular waveform, the main characteristic of monocycle signal is that they have a zero DC component to allow them radiate effectively. The normalized *2nd derivative Gaussian pulse* is expressed as:

$$P_{gauss}(t)=\sqrt{\frac{8}{3\varepsilon}}\left[1-4\pi\left(\frac{t}{\varepsilon}\right)^2\right]e^{-2\pi\left(\frac{t}{\varepsilon}\right)^2} \qquad (12)$$

where ε is a time scale factor and its relation to pulse width T_P is $T_P=7\varepsilon$ which contains 99.99% of the total energy. The corresponding correlation function is found to be as:

$$h_{gauss}(\Delta)=\left[1-4\pi\left(\frac{\Delta}{\varepsilon}\right)^2+\frac{4\pi^2}{3}\left(\frac{\Delta}{\varepsilon}\right)^4\right]e^{-\pi\left(\frac{\Delta}{\varepsilon}\right)^2} \qquad (13)$$

The *normalized Rayleigh pulse* is expressed as:

$$P_{ray}(t)=\sqrt{\frac{8\varepsilon}{\sqrt{2\pi}}}\frac{t}{\varepsilon^2}e^{-\left(\frac{t}{\varepsilon}\right)^2} \qquad (14)$$

and its autocorrelation function can be found as:

$$h_{ray}(\Delta)=\left[1-\left(\frac{\Delta}{\varepsilon}\right)^2\right]e^{-\frac{1}{2}\left(\frac{\Delta}{\varepsilon}\right)^2}. \qquad (15)$$

IV. CAPACITY ANALYSIS OF MULTIUSER UWB

Without loss of generality, let the signals are transmitted in the *l*-th time slot. With perfect synchronization, both the channel delay of τ^1 and time hopping sequence of C_j^1 are known. We also consider that the multiple-access interference is non-Gaussian distributed, yet the number of users in the system is large enough to justify the Gaussian assumption for MAI by invoking the central limit theorem.

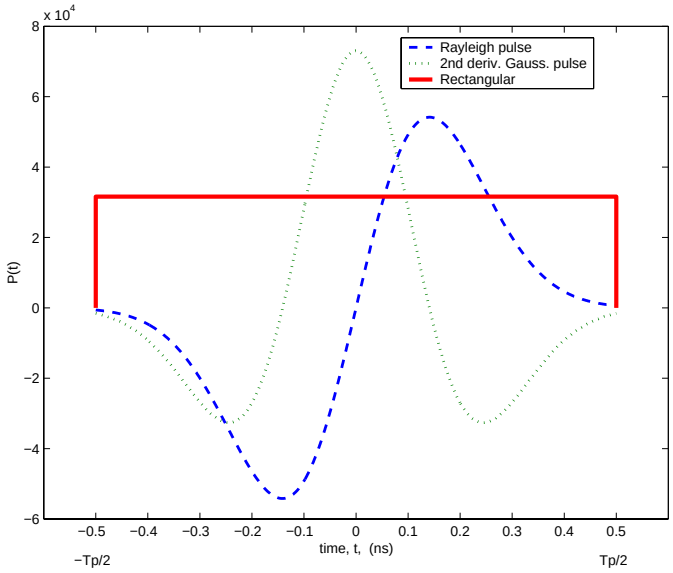

Fig. 4. UWB waveforms with T_P=1ns.

In AWGN, the channel attenuation factor can be assumed as unity, $\alpha=1$, and average SNR per symbol at the output of the correlation receiver is given by:

$$\gamma=\frac{\left(A^1\right)^2}{\sigma_{MAI}^2+Var(N)}=\frac{\left(A^1\right)^2}{\sum_{v=2}^{N_u}\left(A^v\right)^2\left[E\left[h^2(\Delta)\right]-E^2\left[h(\Delta)\right]\right]+\frac{N_0}{2}} \qquad (16)$$

With perfect power control, $A^1=A^v=A=\sqrt{E_P}$, γ becomes:

$$\gamma=\frac{\gamma_0}{(N_u-1)\left[E\left[h^2(\Delta)\right]-E^2\left[h(\Delta)\right]\right]\gamma_0+1} \qquad (17)$$

where $\gamma_0=\frac{2E_P}{N_0}$ is the pulse energy to noise ratio, $E[h(\Delta)]$ and $E\left[h^2(\Delta)\right]$ the first and second moments of the correlation function of the selected pulse waveform, respectively.

The means of $h(\Delta)$, $E[h(\Delta)]$, for rectangular, 2nd derivative Gaussian, and Rayleigh waveforms can be calculated as in the given order as follows:

For rectangular waveform:

$$E[h(\Delta)]=E[h_{rect}(\Delta)]=\int_{-T_P}^{T_P}h_{rect}(\Delta)\frac{1}{2T_f}d\Delta=\frac{1}{2\beta}. \qquad (18)$$

For the 2nd derivative Gaussian waveform:

$$E[h_{gauss}(\Delta)]=\frac{2}{\beta}\left[\frac{\varepsilon}{2T_P}\left(\frac{1}{\pi}-1\right)erf\left(\sqrt{\pi}\frac{T_P}{\varepsilon}\right)\cdots+\left(2-2\left(\frac{T_P}{\varepsilon}\right)^2-\frac{1}{\pi}\right)\exp\left(-\pi\left(\frac{T_P}{\varepsilon}\right)^2\right)\right]. \qquad (19)$$

For Rayleigh waveform:

$$E\left[h_{ray}(\Delta)\right]=\frac{1}{\beta}e^{-\frac{1}{2}\left(\frac{T_P}{\varepsilon}\right)^2} \quad . \qquad (20)$$

Fig. 5 show the autocorrelation functions of the considered waveforms.

The second moments of $h(\Delta)$, $E\left[h^2(\Delta)\right]$ for rectangular, 2nd derivative Gaussian, and Rayleigh waveforms can be calculated as in the given order as follows:

For *rectangular waveform*:

$$E\left[h^2(\Delta)\right]=E\left[h_{rect}^2(\Delta)\right]=2\int_0^{T_P}h_{rect}^2(\Delta)\frac{1}{2T_f}d\Delta=\frac{1}{3\beta} \quad . \qquad (21)$$

For the *2nd derivative Gaussian waveform*:

$$E\left[h_{gauss}^2(\Delta)\right]=\frac{2\varepsilon}{T_P\beta}\left[\frac{1}{\sqrt{2}}\left(1-\frac{1}{\pi}+\frac{35}{96\pi^2}\right)erf\left(\sqrt{2\pi}\frac{T_P}{\varepsilon}\right)+\left(\left(-1-\frac{35}{48\pi^2}+\frac{2}{\pi}\right)\frac{T_P}{\varepsilon}+\left(\frac{8}{3}-4\pi-\frac{35}{36\pi}\right)\left(\frac{T_P}{\varepsilon}\right)^3+\left(-\frac{7}{9}+\frac{8}{3}\pi\right)\left(\frac{T_P}{\varepsilon}\right)^5-\frac{4}{9}\pi\left(\frac{T_P}{\varepsilon}\right)^7\right)e^{-2\pi\left(\frac{T_P}{\varepsilon}\right)^2}\right] \qquad (22)$$

For *Rayleigh waveform*:

$$E\left[h_{ray}^2(\Delta)\right]=\frac{1}{4\beta}\left[\left(1-\left(\frac{T_P}{\varepsilon}\right)^2\right)e^{-\left(\frac{T_P}{\varepsilon}\right)^2}+\frac{3\sqrt{\pi}}{2}\left(\frac{T_P}{\varepsilon}\right)^{-1}erf\left(\frac{T_P}{\varepsilon}\right)\right] . \qquad (23)$$

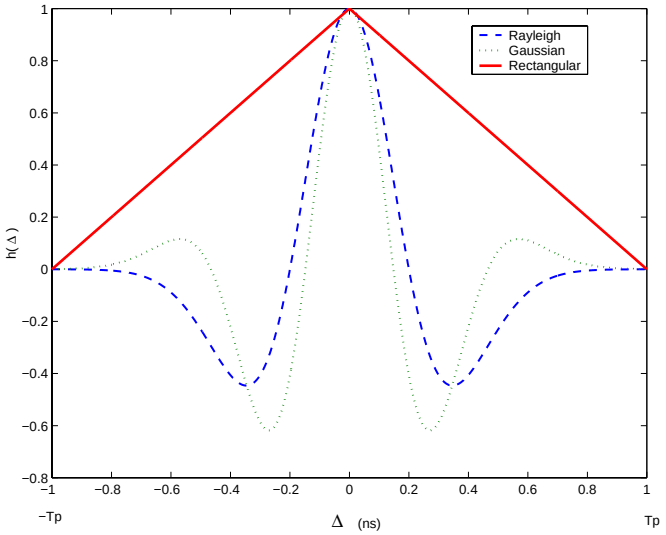

Fig. 5. Autocorrelation of UWB waveforms with T_P=1ns.

With Gaussian approximation for multiuser interference, the expression for single–user capacity (bits/symbol) is defined as [8]:

$$C=\log_2 M-E_{\mathbf{U}|\mathbf{X}_1}\log_2\sum_{m=1}^{M}\exp\left(\sqrt{\gamma}\left(U_m-U_1\right)\right) . \qquad (24)$$

and the random variables U_m, m=1,..,M have the following distributions conditional on the transmitted signal $\mathbf{X}_1$, where $\mathbf{X}$ is interpreted as a collection of points in M-dimensional signal space with one point located on each coordinate axis :

$$\begin{aligned} U_1 &: N\left(\sqrt{\gamma},1\right) \\ U_m &: N(0,1) \quad , \quad m\neq 1 \end{aligned} \qquad , \qquad (25)$$

where $N(\mu,2\sigma^2)$ denotes the Gaussian distribution with mean μ and variance $2\sigma^2$. An analytical study of (29) for a binary PPM (M=2) is presented as a special case in [5]. We consider the channel capacity with respect to pulse waveform of M-ary PPM UWB communications over multiple-access and AWGN channel by using Monte-Carlo simulation of (24).

V. NUMERICAL RESULTS

Several Fig.s are produced to obtain specified results and demonstrate the comparison study of UWB capacity with respect to difference pulse waveforms. Fig. 6 presents the user capacity in bits per M-ary PPM symbol of UWB as a function of number of users for various number of modulation levels M. The curves are obtained by Monte-Carlo simulation with spreading ratio β=10, and noise free channel. Fig. 6 suggests that the UWB user capacity is approximately $\log_2(M)$ for low number of users. Moreover, the user capacity is highly influenced by the shape of the pulse width. Before we go forward to investigate the effect of pulse energy to noise ratio, we need to understand where the capacity difference comes from. The term $\left(E\left[h^2(\Delta)\right]-E^2\left[h(\Delta)\right]\right)$ in (17) represents the variance of the autocorrelation function denoted by σ_h^2. From (18) and (21) for $\beta>>10$, the parameter σ_h^2 for rectangular pulse can be approximated by $\sigma_h^2(rect)\approx\frac{0.333}{\beta}$. The corresponding parameters for the 2nd derivative Gaussian and Rayleigh waveforms with $T_P/\varepsilon=7$ are $\sigma_h^2(2^{nd}\,gauss)\approx\frac{0.14519}{\beta}$ and $\sigma_h^2(ray)\approx\frac{0.095}{\beta}$. We clearly observe that the monocycle waveforms are beneficial in reducing the MAI.

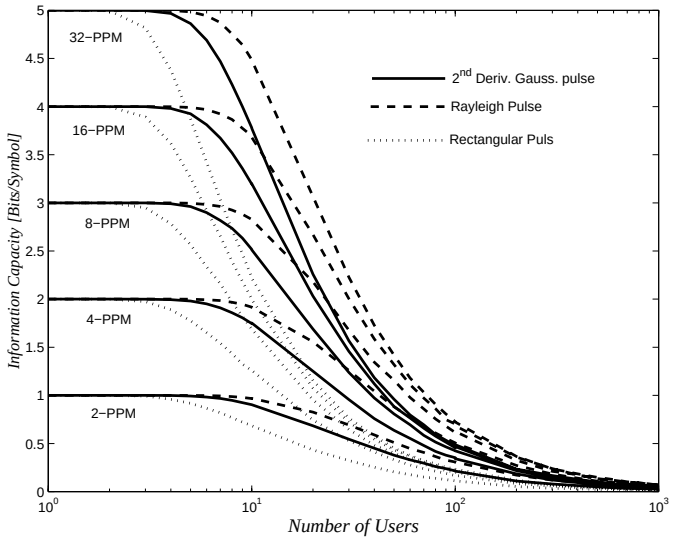

Fig. 6. User information capacity with respect to pulse selection for multiuser UWB, β=10 and noise free channel, $\gamma_0=\infty$.

Fig. 7 presents the capacity in bits per PPM symbols of UWB as a function of symbol SNR for various numbers of levels M with processing gain β=100 and 10 users. Fig. 7 suggests that the UWB user capacity is approximately $\log_2(M)$ for high SNR ranges. The difference between capacity performances of different pulse waveforms is less due to the higher processing gain that minimizes the MAI. Note that in the simulations, the pulse shaping ratio T_P/ε for both the 2nd derivative Gaussian and Rayleigh pulses was loosely selected to be equal to 7. This selection may degrade the performance of the 2nd derivative Gaussian pulse as compared to that of Rayleigh pulse.

It is clear that the pulse shaping ratio is of importance that may influence the capacity performance. Fig. 8 depicts the effect of pulse shaping ratio on the performance of M-ary PPM UWB system. Fig. 8 suggest that the shaping ratio must be greater than 2 and 3 for Rayleigh pulses and the 2nd derivative Gaussian pulses, respectively. Moreover, the performance with Rayleigh pulses can be made equal to that with the 2nd derivative Gaussian pulse by an appropriate pulse shaping ratio.

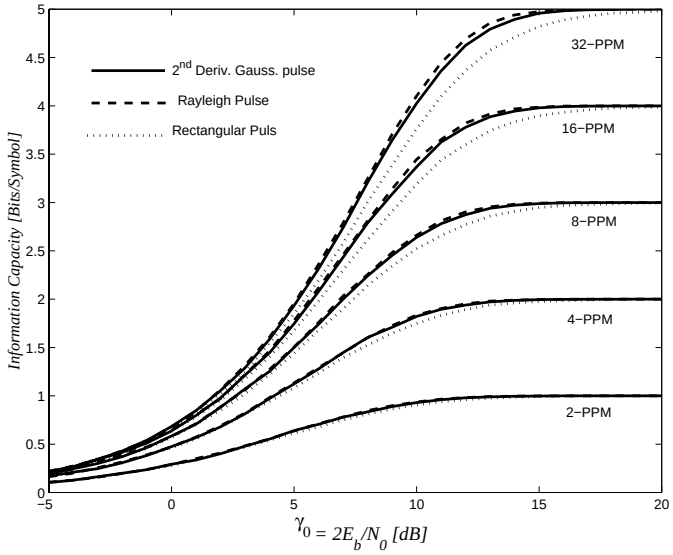

Fig. 7. User capacity versus $\gamma_0=2E_b/N_0$ for multiuser UWB system, 10 users and β=100.

VI. CONCLUSION

In this paper, we have investigated the effect of pulse waveform selection on the information theoretic capacity of the M-ary PPM UWB multiple-access system. Among many practical pulse waveforms, Rectangular, Rayleigh, and 2nd derivative Gaussian pulses are considered. We show that the proper pulse shape selection may result in substantial capacity enhancement as a result of reduction in the MAI. The expressions are generalized for use in multiuser UWB environment with various pulse waveforms. This work can be extended to account for the higher derivative Gaussian pulses adopted by the FCC-2002 regulations.

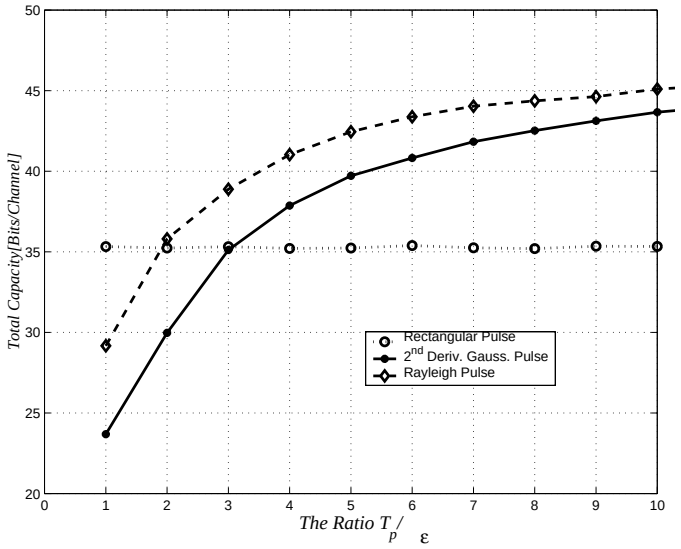

Fig. 8. Total capacity 4-PPM UWB system versus T_p/ε ratio for pulse γ_0=10dB, 50 users and β=100.

REFERENCES

[1] M. Win, R. Scholtz, "Ultra-Wide Bandwidth Time-Hopping Spread-Spectrum Impulse Radio for Wireless Multiple-Access Communications," *IEEE Trans. On Comm.*, Vol. 48, No. 4, pp. 679-691, April 2000.

[2] Federal Communications Commission, "First Report and Order", FCC 02-48, 2002.

[3] Foerster, J.R., "The Effects of Multipath Interference on the Performance of UWB Systems in an Indoor Wireless Channel," *IEEE VTS 53rd Vehicular Technology Conference*, 2001, Spring, vol. 2, pp. 1176-1180.

[4] Lijia Ge, Guangrong Yue, and Sofiene Affes, "On the BER Performance of Pulse-Position-Modulation UWB Radio in Multipath Channels," *IEEE Conference on Ultra Wideband Systems and Technologies*, 2002.

[5] Zhao, L., and Haimovich, M., "Multi-User Capacity of M-ary PPM Ultra-Wideband Communication," *IEEE Conference on Ultra Wideband Systems and Technology*, 2002.

[6] Gryadshteyn I.S. and Ryzhik I.M., Table of Integrals, Series, and Products, 5th ed. San Diego: Academic, 1994.

[7] Conroy, J.L. LoCicero, and D.R. Ucci, "Communication techniques using monopulse waveforms," *IEEE MILCOM' 99*, vol. 2, pp. 1191–1185, 1999.

[8] S. Dolinar, D. Divsalar, J. Hamkins, and F. Pollara, "Capacity of Pulse-Position Modulation (PPM) on Gaussian and Webb Channels," LPL TMO Progress Report 42-142, 2000.